CERN/SPSC 87-47
SPSC/P 234
03.09.1987

PROPOSAL TO THE SPSC

Investigations of the Energy- and Angular Dependence of Ultrashort Radiation Lengths in Si, Ge, and W single Crystals

S.P.Møller, J.B.B.Petersen, A.H.Sørensen, and E.Uggerhøj*
Institute of Physics, University of Aarhus,
DK 8000 Aarhus C, Denmark

K.Elsener**
CERN,
CH-1211 Geneva 23, Switzerland

P.Siffert
Centre de Recherches Nucléaires,
Strasbourg, France

*Spokesman

**Contactman

SUMMARY

The aim of this experiment is to measure for the first time the ultrashort shower formation along crystalline directions of intrinsic semiconductor Si and Ge detectors. Also W-crystals will be used as converter in front of semiconductor detectors.

Very recently two CERN experiments (NA33 and WA81) have shown that pair production by energetic photons incident along crystalline directions is strongly enhanced as compared to the Bethe-Heitler yield for amorphous targets. The enhanced pair production sets in at around 40 GeV in Ge and rises almost linearly with photon energy up to a maximum enhancement of around thirty. In Si, this maximum is nearly two orders of magnitude above the Bethe-Heitler value.

For GeV electrons/positrons incident along crystal axes, the radiation energy loss also show very large enhancement of approximately two orders of magnitude. In a 0.4 mm W crystal a 100 GeV electron will emit on average 70% of its total energy.

The combination of the dramatic enhancements for radiation and pair production means that the electromagnetic shower develops (10-50) times faster corresponding to ultrashort radiation lengths around crystalline directions.

If semiconductors (Si,Ge) crystals are used as converters the ionization energy loss from the pairs is measured immediately. In other cases the converter crystal can be mounted in front of a semiconductor detector.

By this technique very thin (mm) and compact shower detectors can be constructed for the energy region above ~50GeV. The angular resolution is around 1 mrad and the hadron background is reduced drastically inside this angle cone. Such detectors could be of interest as compact electromagnetic calorimeters in collider and fixed target experiments and could also be used in gamma-astronomy to locate with high angular resolution the sources of TeV γ-rays in the universe.

A beam divergence smaller than the critical angle for channeling (~50μrad) will give the possibility to investigate the discriminatory manner in which the crystal converter interacts with electrons and positrons. This could lead to a gamma detector with an angular resolution even in the 50μrad-region.

Beam and Beamtime

The investigations of "hard" and "soft" showers require a range of electron/photon energies from ~20 GeV to the maximum available. The beam should be collimated to around 50 μrad or less. The intensity should be low ~10^3/sec to prevent pile-up in the solid state detectors. The experimental setup containing drift chambers, goniometer, target chamber, etc. is already existing. A beam time of around 10 days is estimated, preferably with some interruption in the middle of the run.

I. PHYSICS BACKGROUND

In this chapter an introduction to the physics around pair production and radiation in single crystals at multi-GeV energies is given. For a quick overview of the subject, the reader is referred to the attached article from Nature.

The process of $e^{\pm}$ pair production (PP) is very closely related to the process of bremsstrahlung (BS). If PP is viewed as the excitation of an electron from a state of negative energy to one with positive energy by an incoming photon in the field of an atomic nucleus, which is needed to ensure energy and momentum balance, the reverse process is emission of bremsstrahlung through scattering in the atomic field with the electron ending up in a negative energy state. Because of this symmetry, PP and BS are usually treated in parallel in the literature[1,2], the cross sections differing only because of difference in density of final states. As an introduction to the discussion of the coherence effects which may appear in PP when photons are incident on a single crystal at small angles to a crystallographic axis, it may be instructive first to consider the corresponding well-studied cases of coherent bremsstrahlung and channeling radiation.

Bremsstrahlung and channeling radiation

When a parallel beam of electrons or positrons traverses a crystalline target in directions far from crystalline axes and planes, the well known one-atom incoherent bremsstrahlung (IBS) is emitted which, at high velocities and for not too high atomic charges, Z, is well described by the Bethe-Heitler formula. As the direction of incidence moves towards planar directions, the projectile feels the crystalline structure, and coherence in the successive interactions occurs, resulting in the interference structure of coherent bremsstrahlung (CBS) (for a review see Ref.2). The peak energies are closely related to the lattice constants and the incident angle with respect to the crystal planes.

If the direction of incidence is nearly parallel to axial or planar directions, the projectile motion becomes governed by the lattice continuum potential obtained by smearing the atomic charges along axes or planes. The resulting strong steering effect is known as <u>channeling</u>[3,4,5]. This special motion gives rise also to coherence effects, and the ensuing radiation is called <u>channeling radiation</u> (ChR)[6,7,8]. The structure of ChR is strongly connected to the form of the trapping potentials but is not (as is CBS) directly connected to the lattice parameters. In the channeling picture, positrons are pushed away from atomic axes and planes, whereas electrons are focused around the nuclei. The two types of particles therefore "see" different potentials, and their ChR spectra will be different in shape, which is not the case for CBS.

For IBS and CBS emitted by GeV electrons, a first-order Born approximation is applicable for not too high Z-values. This means that the scattering in the atomic field as well as the interaction with the radiation field is treated as perturbations, leading to a two-vertex process. However, in the channeling case, the perturbative treatment of the interaction with the crystal field breaks down. As opposed to IBS and CBS, channeling radiation is a one-vertex process since only the interaction with the radiation field can be treated as a perturbation.

In Fig.1 are shown typical intensity spectra of high-energy incoherent (a) and coherent (b) bremsstrahlung. The interference structure of CBS is clearly evident from the figure, whereas IBS-spectra are smooth. In Figs. 1c and d are shown ChR spectra for 7 GeV/c positrons (c) and electrons (d) incident on a 100 μm thick silicon crystal along the (110) planar direction. The ChR is confined to the lower part of the spectrum, where an enhancement over IBS of nearly two orders of magnitude is observed. The peak structure observed for positrons appears since positive projectiles feel a nearly harmonic planar continuum potential. As inserts in Fig.1c and 1d are shown angular distributions of ChR for those projectiles which emit photons with energies of 10-40 MeV. Here it is obvious that the channeling effect sets in abruptly for incident angles ψ of the order of the critical angle for planar channeling ψ_p, i.e., for $\psi < 50$ μrad, with respect to the (110) plane.

Figs 1 e and f show ChR-spectra for 10 GeV/c electrons/positrons incident along the <110> axis in a 100 μm thick Si crystal. In both cases the spectra are structureless due to the anharmonic axial potential for both electrons and positrons. The ChR is strongly enhanced over the incoherent yield. The reduction in yield for low energy photons is due to the so-called Landau-Pomeranchuk effect. The incident angles cover $(0.5\text{-}1.0)\psi_1$, where ψ_1 is the characteristic axial channeling angle given by:

$$\psi_1 = \sqrt{\frac{4Ze^2}{pvd}} \tag{1}$$

where Z is the atomic number of the target, p and v projectile momentum and velocity, respectively, and d the lattice spacing along the axis.

In order to describe GeV-channeling, classical relativistic mechanics can be used due to the many quantum states in the transverse phase space[4]. For particle energies up to 5-10 GeV the coherent part of the photon spectrum only reaches up to around 20% of the projectile energy. This means that the recoil of the projectile during radiation emission can be neglected and together with the many quantum states ChR in the few-GeV region appears as a classical emission process described by classical electrodynamics.

Very High Energies - and Pair Production

For incidence energies of several tens of GeV, the classical description of channeling radiation becomes invalid. Clearly, the problem here is not a quantization of the transverse motion of the charged particle. Instead, the breakdown is associated with the recoil due to the emitted photon. The photon energy amounts to an appreciable fraction of the primary energy and cannot be neglected as in a classical treatment.

However, at these high impact energies another simplification applies: The range of photon emission angles ($\sim 1/\gamma$) relative to the local particle direction of e.g., an axially channeled electron or positron, is small compared with the excursions in projectile angle relative to the axis, $1/\gamma \ll \psi_1$ ($\propto 1/\sqrt{\gamma}$). Consequently, the transverse distance travelled by the projectile during coherent photon emission is small compared with distances over which the continuum potential, or rather its derivative, varies significantly. The emission appears as in a constant electromagnetic field, a case treated in great detail in the literature and known as synchrotron radiation[9]. To obtain the channeling radiation spectra it then suffices simply to compute those of synchrotron radiation corresponding to the various field strengths encountered in a channel and then make an average. Figure 2a shows theoretical spectra obtained in this way with an averaging corresponding to equal probability everywhere in the channel[9b]. The yield has been normalized to that of incoherent bremsstrahlung. Clearly, positrons, being concentrated in the region of low field strengths, will show somewhat lower yield and photon energies than displayed in the figure whereas electrons give higher yields and energies. Channeling shows up only as a focussing or defocussing effect - exactly as in the traditional channeling experiments. In fig.2b[10] are shown radiation spectra from 100 GeV to 800 GeV electrons incident on a <110> W-crystal at 293K. It should be noticed that for high impact energies the photon spectra becomes nearly constant. By this effect it is possible to enhance dramatically the production of hard photons. Above 800 GeV the spectra even peak at the maximum photon energy.

Quantum mechanically, the treatment of the process where an energetic photon converts into an electron-positron pair in the field of, e.g., an atomic nucleus, which is needed to ensure energy-momentum balance, is identical to that of bremsstrahlung with a few nearly trivial exceptions. Consequently, the various radiation modes discussed above are parallelled by similar pair production mechanisms.

In PP the opening angle of the pair is of order $1/\gamma$. For channeling to influence the process, through capture into channeled orbits of the charged particles produced by a photon incident along, e.g., a major crystallographic axis, it is necessary that the opening angle is smaller than the critical channeling angle, $1/\gamma<\psi_1$. This leads to a threshold in photon energy of

$$\hbar\omega_{th} \simeq 2mc^2 \frac{mc^2}{|U(0)|} . \qquad (2)$$

A typical value for, e.g., silicon is 5 GeV. However, in order to compete with incoherent pair production it is necessary to go considerably higher in energy (see also next page).

In the multi-GeV region it is possible to make use of the fully developed theory for pair production in strong, constant electromagnetic fields (C.F.A.). From this the differential pair production yield for photons of energy $\hbar\omega$ is given by

$$\frac{dW}{d\eta} = \frac{\alpha}{\sqrt{3}\pi\lambda} \frac{mc^2}{\hbar\omega}\left[\frac{1}{\eta(1-\eta)}K_{2/3}(\xi)-\int_\xi^\infty dt K_{5/3}(t)\right] \qquad (3)$$

$$\xi = \frac{\alpha}{3\eta(1-\eta)\varkappa}; \qquad \varkappa \equiv |V'|\frac{\lambda}{mc^2}\frac{\hbar\omega}{mc^2}; \qquad \eta \equiv \frac{E_+}{\hbar\omega}$$

where α is the fine structure constant, $\lambda = \hbar/mc$ the Compton wavelength of the electron, E_+ the positron energy and $K_{n/3}$ a modified Bessel function of order n/3.

In fig.3a are shown calculated coherent pair-production yields (full drawn) for 100-GeV photons incident near the <110> axis in Ge. The dashed curve shows the spectrum of one of the emitted charged particles obtained from eq.3 for 100 GeV photons incident along the <110> axis of a germanium single crystal. The dotted curve indicates the incoherent rate and, clearly, a strong enhancement is observed. For the coherent pair production incidence in the (100) plane is assumed. At the present impact energy the spectrum corresponding to the lower angle is quite similar to the constant field result.

In fig.3b are shown total yields of pairs from photon conversion along the strongest axis in various crystals as function of incident photon energies.

In the theory of Baier et al.[11] simple analytical estimates for maximum enhancements in pair production are given, i.e.

$$r^{max} \equiv \frac{W^{max}}{W_{BH}} \sim \frac{1}{3} \frac{a_s m}{Z\alpha \ln(183 Z^{-1/3})} , \qquad (4)$$

where a_s is the screening parameter for the continuum potential. This shows that in diamond the axial pair production is more than two orders of magnitude larger than the Bethe-Heitler yield.

Simple estimates[11] are also given for the photon energies at which the axial pair production becomes noticable, i.e.

$$\hbar\omega \sim \frac{m^3 \varrho d}{Z\alpha}, \qquad (5)$$

where ϱ is thermal vibrational amplitude. From (4) and (5) it is clear that low threshold energies require heavy elements like W but the enhancements are then less pronounced.

The parameter relevant for applications is $\hbar\omega_t$, which is the photon energy for which the pair production along a crystal axis equals that in an amorphous target of the same thickness (Bethe-Heitler). This parameter is tabulated in ref. 22.

Angular Dependence of High-Energy Radiation and Pair Production

The transition with decreasing incidence angle from coherent pair production towards the region where the constant field approximation applies contains some surprises. From simple arguments on the transverse length scale involved in the production process one is led to the result that the latter may be employed for angles up to an energy independent limit of approximately

$$\theta_0 = \frac{|U(0)|}{mc^2} . \qquad (6)$$

Above threshold, (eq.(5)), this angle is large compared with the critical channeling angle which decreases with increasing energy, $\psi_1 \propto \gamma^{-1/2}$. Hence the question whether the produced pair is channeled appears not to be decisive, which was believed in the first case. Even more surprising at a first glance may be the fact that applicability of the constant field approach out to θ_0 implies a break-down of the perturbative coherent pair production computations at angles smaller than θ_0 (ref.23). The break-down appears at high energies since characteristic angles scale as $1/\hbar\omega$. This is in contrast to the result obtained at, e.g., MeV impact energies where the coherent scheme in the case of radiation successfully may be applied all way down to ψ_1. However, a closer analysis shows that applicability of the perturbative approach, which produces, e.g., identical radiation spectra for electrons and positrons, requires the deflection angles of the charged particles to be small compared with $1/\gamma$, the opening angle of the photon or pair production cone[23]. This is exactly equivalent to the condition $\theta > \theta_0$. The cut at θ_0 implies a saturation of rates at ultra-high energies. Note that a typical value of θ_0 for axial cases is ~1/2 mrad (Ge<110>).

Although the angular dependence of both PP and radiation scale with θ_0, the actual angular width of the radiation peak is smaller than for PP.

Shower Formation

In the last years different groups have started programs to calculate the combined effects of the strong enhanced radiation and pair production along crystalline axes and planes[19,20]. The possibility of using single crystals for shower formation in detecting the angular variation of incident gamma-rays in the GeV-TeV region has been proposed[21,22].

Out of these investigations have appeared some very interesting results. In fig.8a[20] is shown calculated radiation length along axial directions in Si and Ge single crystals as a function of photon energy. Clearly the axial radiation lengths are energy dependent in contrast to amorphous materials and reduced (10-50) times. For 100 GeV <110> Ge L_{ch} is only ~1mm as compared to ~20 mm amorphous Ge. So in a few cm of crystalline Ge most of a shower will develop. The threshold energy $\hbar\omega_t$ for pair production parts up the shower in two different types, namely: 1) the "hard" showers for $\omega \gg \omega_t$, where both radiation and pair production is enhanced and 2) the "soft" showers, $\omega < \omega_t$. In the soft showers, the pairs are produced by the normal Bethe-Heitler mechanism, but the charged particles emit a large number of soft photons, resulting in an increased number of electrons/positrons. In the soft showers, however, there will be many more photons than charged particles.

In fig.8b[20] is shown the number of photons (N_γ) and the number of electrons (N_e) at a depth of 1 cm in a <110> single Si crystal as a function of photon energy. It should be noted that N_γ/N_e is practically constant and equals 11. This means that the photon energy can be measured over an enormous energy range just by measuring the number of charged particles. For 200 GeV photons estimates show that in a 1 mm thick W-crystal around 5 electrons are produced in a random direction but around 20 electrons in an axial direction[20].

The angular dependence of the enhanced shower formation around a crystal axis should vary with a characteristic angle of the order of $\theta_0 \sim 1$mrad and not the critical channeling angle $\psi_1 \sim 50$ μrad.

II. PRESENT EXPERIMENTAL SITUATION

Pair Production

Until now only three experiments have been performed, all at CERN, two in the North Hall (NA33) and one in the West Hall (WA81). The data analysis for WA81 is not fully completed, but the general behaviour has come out, so we show preliminary results here for a comparison with the NA33 results.

In the first experiment (NA33) performed to investigate the influence of the crystal lattice on multi-GeV pair production[14] severe discrepancies from theoretical predictions of the yield were encountered. Furtheron, a dip appeared around $\sim\psi_1$. A recent second experiment (NA33)[15] obtained much better agreement with theory and, by washing out the dip at ψ_1, it seems to support the hypothesis of applicability of the constant field approximation out to $\sim\theta_0$. Since photons do not get focussed, as opposed to the charged projectile in the radiation process, the yield appears in this approximation essentially constant out to the latter angle. In fig.4 is shown the results from the first and second NA33 experiment together with the results from our own experiment (WA81). Clearly our results agree with the second NA33 experiment. The WA81 results are compared to calculations using the Baier et al. theory[11] and using a Doyle-Turner approximation for the continuum potential including thermal averaging. The agreement between the two last experiments (NA33 and WA81) and theoretical prediction is good.

The angular dependence of the enhancements is shown in fig.5a (NA33) from which it is seen that the θ_0 is the characteristic angle for constant field effect and not the channeling angle ψ_1, which in the present energy regime is 10-20 times smaller. The analysis of our data from WA81 also agree with the second NA33 results as can be seen from fig.5b.

The fact that θ_0 and not ψ_1 is the characteristic angle means that crystalline materials with some mosaic spread can be used. This means that a whole new array of materials becomes available for experiments - especially interesting are the high-Z (W, Ir, Re, Os) and low-Z (diamond) elements (eqs.4 and 5).

Radiation

The inverse pair production process, namely radiation from (100-200) GeV electrons and positrons incident along crystalline directions was only investigated very recently. Both NA33 and WA81 have taken data in this regime. The NA33 data[16] are shown in fig.6 together with our WA81 results for 170 GeV electrons incident on Ge and Si crystals. The most surprising observation is the high photon peak at 0.85 E_0 in the NA33 electron data. At first one would think of a multiphoton effect, because the crystal thickness corresponds to around 1% radiation length in a random direction and along axial directions the radiation intensity is enhanced (10-50) times. On the other hand, the NA33 multiplicity measurements apparently rule out this possibility. In the WA81 results, no such sharp peak is seen. Note however, that a comparison is difficult, because the Ge crystal in WA81 was three times thicker. In WA81 we also used a 0.5 mm <110> Si crystal which only corresponds to 0.5 % radiation length in a random direction. The spectra are also shown in fig.6. Unfortunately the statistics only allow to integrate the photon yield from an incident angular region of 0-ψ_1 around the <110> axis. In this angular region no distinct peak is seen - only a strong enhancement, which is expected. The NA33 data, on the other hand, show a strong intensity variation by tilting the crystal 17 μrad in a beam divergence of $\pm$30 μrad. This fact means that the alignment is very critical. In the WA81 results the true alignment could be ~(15-20) μrad off; this is currently under investigation. On the other hand, the total radiated energy shows a dip for positrons and a peak for electrons (fig.6d). This difference, which is due to axial channeling, occurs for incident angle smaller than ψ_1 ~ 50 μrad, so the actual alignment is close to the axis.

In fig.7a[17] are shown calculated and measured total radiative energy losses for Si, Ge, and W crystals as function of crystal thickness. The curves are given for different temperatures and electron energies between 100 GeV and 200 GeV. In the calculations the recoil effects are taken into account. Clearly the radiation enhancement is very large and in only 0.4 mm W crystal around 80% of the total energy is lost. The angular dependence of the total emitted radiation for 150 GeV electrons and positrons incident close to the <110> axis in a Ge crystal cooled to 100K is shown in fig.7b[22,18]. Curve I is calculated using the constant field approximation and particle flux redistribution in the crystal due to channeling. The curves show the two characteristic angles (ψ_1 and θ_0) for channeling and constant field approximation, respectively.

III Compact Electromagnetic Calorimeter and TeV-Astronomy

The dramatic reduction of radiation lengths (10-50 times) at high energies along crystalline directions open very exciting new experimental possibilities. The angular resolution in GeV gamma ray telescopes can be increased by one to two orders of magnitude[21,22] to around a mrad. Furthermore, compact electromagnetic calorimeters for very high energies can be envisaged, with an angular acceptance of a few mrad. As mentioned previously, the very large reduction in the radiation length only occurs at high energies (above some tens of GeV), where both the pair production and the radiation is enhanced. At lower energies only the radiation is increased, and only a smaller reduction in the radiation length can be expected. A calorimeter for very high energies could thus consist of a crystal converter, transforming the incoming particle to a soft shower, followed by a normal calorimeter for low energies. Also a sandwiched calorimeter, with semiconductor detectors as the active material and aligned crystals as the showering material can be envisaged. Such calorimeters has been demonstrated for amorphous materials[24]. The fact that the electromagnetic radiation length is reduced by 1-2 orders of magnitude at high energies, whereas the hadronic interaction length is unchanged, greatly improves the e/γ-hadron separation at very high energy. The acceptance of such calorimeters, if placed at a distance of a few meters, can cover the interaction region of both colliding e^+/e^- beams - and fixed target - experiments.

Especially interesting is the case where intrinsic semiconductor detectors are used both as converters and to detect the charged particles from the shower. In a semiconductor detector the energy resolution is very good and the number of charged particles in the shower can be measured with a large accuracy. In 1mm of Ge and Si the random energy loss for minimum ionising particles is ~500 keV and ~300 keV, respectively, so large signals can be expected. Semiconductor detectors have also the advantage of not requiring much power which is expecially important for satellite flown detectors. Furtheron, the total weight of such a shower detector is minimal.

IV THE PROPOSED EXPERIMENT

It is proposed to investigate in detail the shower formation in single crystals of Si, Ge, and W. The three types of crystals are expected to have very different enhancements for pair production (eq. 5) and different thresholds (eq. 6) for onset of the effects. The angular dependence of the enhanced effects is also expected to vary. Another aim of the experiment is to find the optimal thickness for which multiple scattering is minimal (giving best angular resolution), and where the differences in axial and random signals are most pronounced. In order to investigate the transition region from "soft" to "hard" showers, it is important to have electron/photon energies as high as possible and to be able to vary the beam energy.

In order to investigate the development of showers along crystalline directions, the number of photons and charged particles should be measured for varying thickness of the converter crystal. The value of the different parameters can directly be compared to those predicted by the cascade calculations by Baier et al[20] (fig. 7 and 8).

The number of charged particles behind the crystal converter will be measured by a Si semiconductor detector. The number of photons will be estimated by a sandwich-type calorimeter, also used to measure the total radiated energy.

Experimental Considerations

The beam line

For the investigations is needed an electron/photon beam with energies up to around 200 GeV or more. The angular divergence should be 50 μrad or better. The intensity should be rather low: 10^2-10^3 particles/sec - not to produce pile-up in the solid state detectors. In fig.9 is shown a layout of the experimental setup. A bending magnet is needed to dump the electron beam away from the photon detector positioned in the forward direction. A beam diameter of less than ~10 mm is required for our crystal converters and semiconductor detectors.

The targets

The targets will be Si, Ge, and W single crystals with thicknesses in the mm range. The crystals are first tested for bending and mosaic spread and cut with preferred crystal orientation. The targets are mounted in a highly stabilized channeling goniometer, where cooling to around 90K is possible.

The goniometer is mounted in our channeling vacuum chamber on which high resolution drift chambers are mounted. Alignment and target spots can be controlled on-line by the drift chambers. The detailed scanning is performed by the goniometer. Behind the goniometer is mounted the Si semiconductor detector used to measure the number of charged particles in the shower.

In order to prevent bending due to cooling, the crystals are fixed at the top with glue in only one point and thereby hanging free. This technique has until now given nearly strain free mountings. In the case of Si and Ge, the converter crystals can in principle act as intrinsic detectors and at the same time detect the number of charged particles.

Angular resolution

The angular spread of the electron/photon beam is expected smaller than 50 μrad. The goniometer has a step-angle variation of 10 μrad, which should be compared to the characteristic angle for the crystal effect of $\theta_0 \sim 1$ mrad and the critical angle for channeling $\Psi_1 \sim 50\mu$rad. As pointed out above, the shower formation could be influenced by the very different way in which channeled electrons and positrons interact with the converter crystal: channeled electrons are focused around the nuclei, whereas channeled positrons are repelled from the nuclei. This gives rise to large differences in processes like multiple scattering and ionization - and radiation - energy losses.

Crystal alignment

The crystals will be aligned by using the well known channeling radiation. The electrons are swept out of the photon beam by the bending magnet BM2. The photons are detected by an array of lead-glass detectors.

Photon Detector

We plan to use a sandwich-type calorimeter (Si/W or scintillator/lead) to detect the total energy of the photons in the cascade. This calorimeter will also give information about the number of photons, and could at a later stage be modified to a prototype of a compact electromagnetic calorimeter by using aligned crystals as converting material.

Data-taking and running time

The event structure in the present experiment is very simple and will be written on tape using a small computer. Since optimal crystal thicknesses have to be found experimentally, the total running time is hard to estimate beforehand. One week of beam-time in the beginning would be suitable.

References

1) J.M.Jauch and F.Rohrlich, The Theory of Photons and Electrons, Springer Verlag, New York, 1980
2) G.Diambrini Palazzi, Rev.Mod.Phys.40 (1968) 611
3) D.S.Gemmell, Rev.Mod.Phys.46 (1974) 129
4) E.Uggerhøj, Phys.Scripta 28 (1983) 331
5) A.H.Sørensen and E.Uggerhøj, Nature 325 (1987) 311
6) V.V.Beloshitsky and F.F.Komarov, Phys.Rep. 93 (1982) 117
7) J.U.Andersen, E.Bonderup and R.H.Pantell, Ann.Rev.Nucl.Part.Sci.33 (1983) 153
8) A.W.Sáenz and H,Uberall, Coherent Radiation Sources, Springer Verlag, Heidelberg, 1985
9) L.D.Landau and E.M.Lifschitz, Course of Theoretical Physics Vol.4., Pergamon Press, Oxford, 1971; J.C.Kimball & N.Cue, Phys.Rep. 125 (1985) 69-101
10) V.N.Baier, V.M.Katkov, and V.M.Strakhovenko - private communication
11) V.N.Baier, V.M.Katkov, and V.M.Strakhovenko, Nucl.Instrum.Methods B 16 (1986) 5
12) J.C.Kimball, N.Cue, L.M.Roth, and B.B.Marsh, Phys.Rev.Lett. 50 (1983) 950
J.C.Kimball and N.Cue, Nucl.Instrum.Methods B 2 (1984) 25
N.Cue and J.C.Kimball (ibid) 29
13) A.H.Sørensen, E.Uggerhøj, J.Bak, and S.P.Møller, Phys.Scripta 32 (1985) 149
14) A.Belkacem et al. Phys.Rev.Lett. 53 (1984) 2371 erratum: Phys.Rev.Lett. 54 (1985) 852
15) A.Belkacem et al. Nucl.Instrum.Methods B 13 (1986) 9
A.Belkacem et al. Phys.Rev.Lett. 58 (1987) 1196
16) A.Belkacem et al. Phys.Rev.Lett. 25 (1985) 2667
A.Belkacem et al. Phys.Lett. B 177 (1986) 211
17) V.N.Baier, V.M.Katkov, and V.M.Strakhovenko, Phys.Lett. 114A (1986) 511
18) V.N.Baier, V.M.Katkov, and V.M.Strakhovenko, Phys.Lett. 117A (1986) 251
19) A.I.Akhiezer and N.F.Shulga, Sov.Phys.JETP 58 (1983) 55
20) V.N.Baier, V.M.Katkov, and V.M.Strakhovenko, Nucl.Instrum.Methods B 27 (1987) 360
V.N.Baier, V.M.Katkov, and V.M.Strakhovenko: The study of particles having very high energy in oriented single crystals (in russian), Novosibirsk preprint 86-115

21) B.McBreen, Astron.Express 1 (1984) 105
22) V.N.Baier, V.M.Katkov, and V.M.Strakhovenko, Nucl.Instrum.Methods A 250 (1986) 514
23) A.H.Sørensen in Proc.Workshop on Relativistic Channeling, Acquafredda di Maratea, Italy 31.3.-4.4. (Plenum, in press)
24) G.Barbiellini et al., Nucl.Instrum.Methods A 235 (1985) 55, A 235 (1985) 216, A 236 (1985) 289 and A 236 (1985) 316

Figure Captions

Fig.1. (a) The incoherent bremsstrahlung spectrum for different electron energies in MeV as a function of the photon energy in units of the incident electron energy. (b) Measured and calculated coherent bremsstrahlung spectrum for 4.8 GeV electrons incident on a diamond crystal (Ref.2). (c) Measured and calculated radiation from planar channeled 7 GeV positrons and electrons (d) in a 0.1-mm Si crystal normalized to IBS. Channeling radiation from 10 GeV electrons and positrons (e) incident along the <110> axis in a 100 μm thick Si crystal. The incident angle region covers $(0.5\text{-}1.0)\psi_1$.

Fig.2. (a) Channeling radiation in the synchrotron (constant field) approximation for incidence along the <110> axis in silicon. Only the coherent part of the spectrum is displayed. (b) Similar spectra for 100 to 800 GeV electrons incident along the <110> axis in a W crystal at 293K.

Fig.3. (a) Differential CPP (full drawn) CFAPP (dashed) and BH (dotted) yield for 100 GeV photons incident at an angle θ to the <110> axis in germanium at a target temperature of 100K as a function of η. For CPP incidence in the (100) plane is assumed. (b) yield of pairs from converted photons along the strongest axis in various crystals as a function of incident photon energy. The yields are given relative to the Bethe-Heitler yield. Crystal temperatures are 100K. For the calculations the C.F.A. is used.

Fig.4. Pair production yield as function of photon energy for photons incident along the <110> axis in Ge. Results are shown for both the NA33 and the WA81 experiment.

Fig.5. Angular dependence of total pair production yield around the <110> axis in a 1.4 mm thick Ge crystal[15]. The solid curves are calculated from C.F.A. and the dashed curves are calculated using the Born

approximation.

Fig.6. (a) Radiation spectrum for 150 GeV electrons incident along the <110> axis in a 0.185 mm thick Ge crystal, (NA33)[16] results. (b)(c) Radiation spectra along the <110> axis in a 0.5 mm Ge (b) and a 0.5 mm thick Si (c) crystal.

Fig.7. (a) The average relative energy losses of an electron as a function of crystal thickness[17]. The curve numbers correspond to: (1) <111> Si, T=293K, ε_0=200 GeV; (2) <110> Si, T=293K, ε_0=200 GeV; (3) <110> Ge, T=280K ε_0=150 GeV; (4) <110> Ge, T=100K, ε_0=150 GeV. (5) <110> Ge T=100K, ε_0=200 GeV; (6) <111> W T=293K, ε_0=100 GeV; (7) <111> W T=77K, ε_0=100 GeV; (8) <110> Ge, T=100K, ε_0=150 GeV - but in the calculations the <u>classical</u> formulas are used. (b) Angular dependence of emitted radiation from 150 GeV electrons incident on a thin <110> Ge crystal at 100K. Curve I is calculated using C.F.A. and II is the coherent bremsstrahlung. For small incident angles channeled positrons (1) and electrons (3) give large differences in emitted intensities due to the steering from channeling.

Fig.8. Calculated radiation lengths[20] in Si and Ge single crystals as a function of incident photon energy. (1) <111> Si T=293K, (2) <110> Si, T=293K, (3) <110> Ge T=280K, (4) <110> Ge T=100K. (b) Total number of charged particles (N_e) and photons (N_γ) with energies above 100 MeV as a function of photon energy. The converter crystal was a 1cm thick <110> Si with T=293K. The ratio N_γ/N_e is practically constant and equal to 11.

Fig.9. Experimental layout. The magnet BM1 cleans the electron beam from background photons. A vacuum system will be installed between BM1 and the driftchamber (DC1) in front of BM2. SC is a beam-defining scintillator. The targets are SI, Ge and W crystals, mounted on a goniometer. A semiconductor detector

is used to measure the number of charged particles produced in the crystal. BM2 sweeps electrons and positrons out of the forward direction, in which a sandwich-type photon detector is situated.

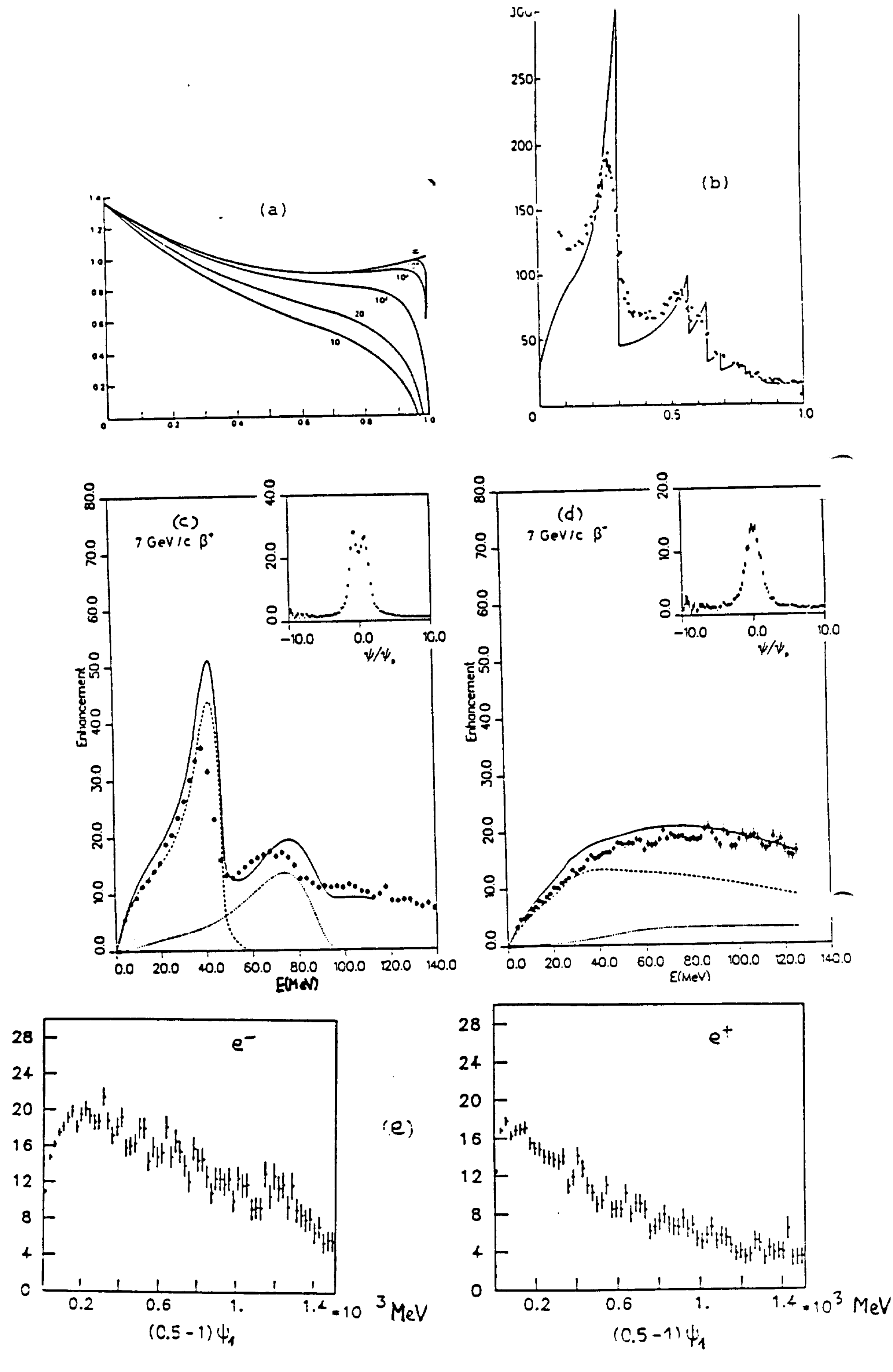

Fig. 1

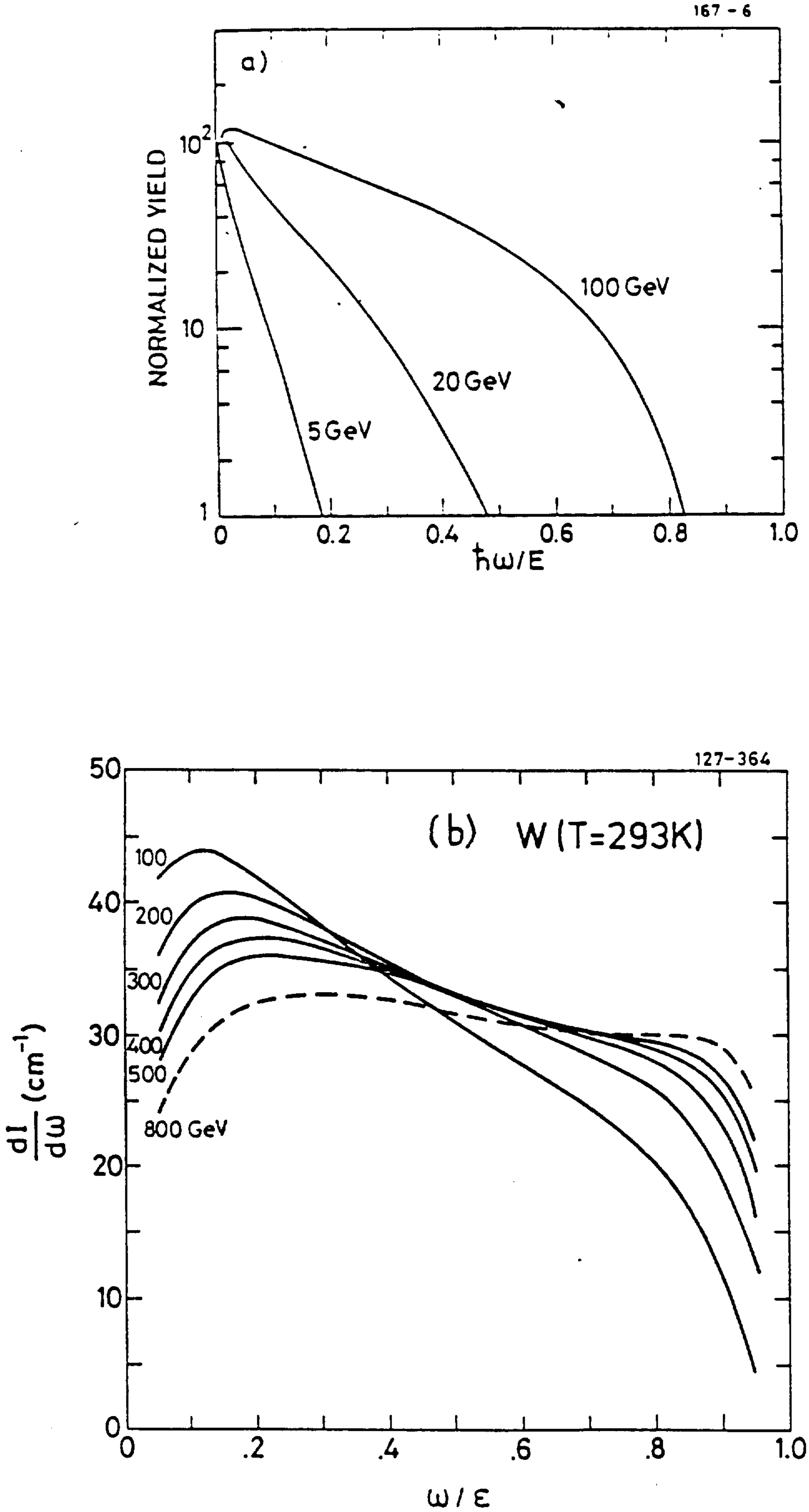
167 - 6
a)
NORMALIZED YIELD
10^2
10
1
100 GeV
20 GeV
5 GeV
0
0.2
0.4
0.6
0.8
1.0
ħω/E
127-364
(b) W (T=293K)
50
40
30
20
10
0
100
200
300
400
500
800 GeV
dI/dω (cm^-1)
.2
.4
.6
.8
1.0
ω / ε

Fig. 2

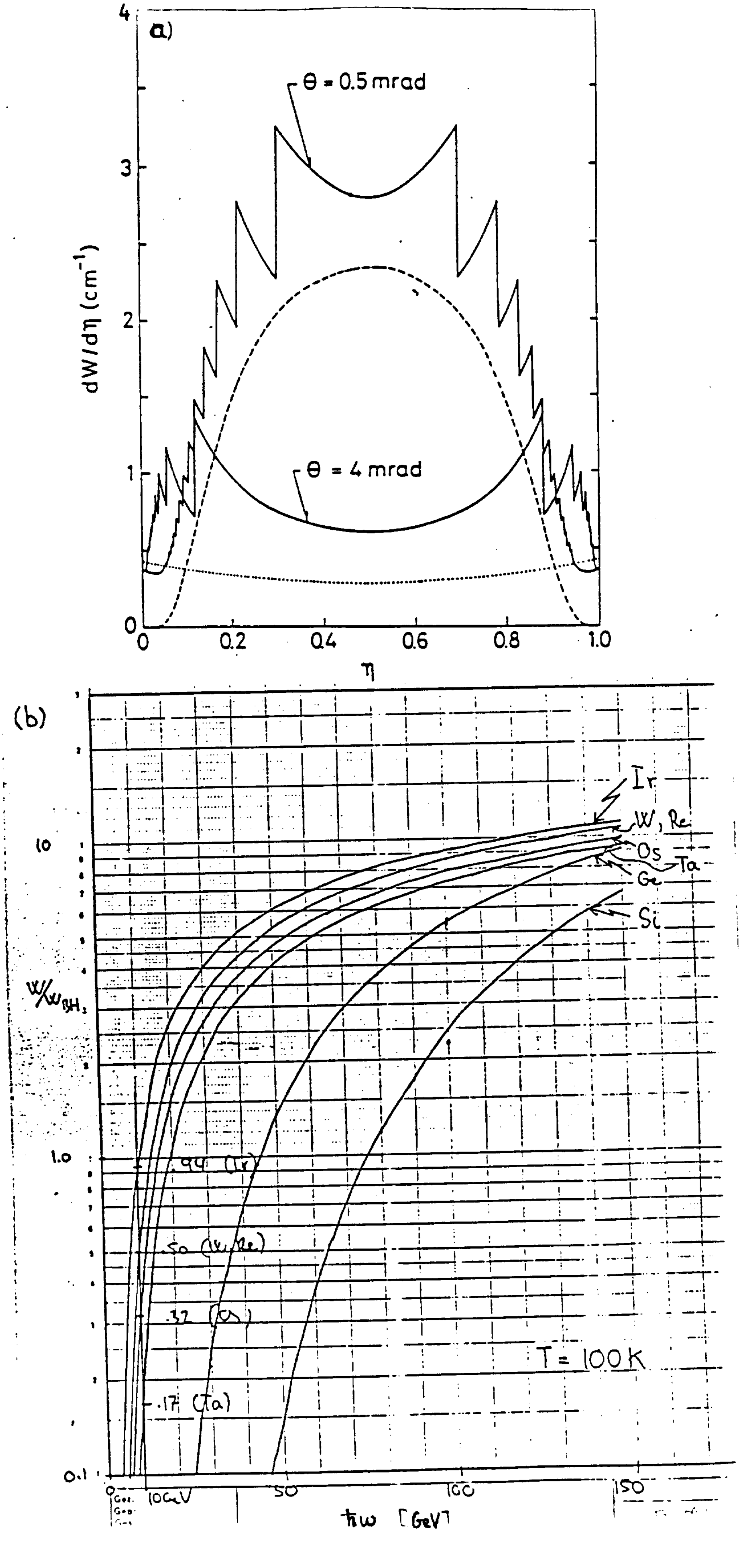
a)
θ = 0.5 mrad
θ = 4 mrad
dW/dη (cm⁻¹)
η
(b)
Ir
W, Re
Os
Ta
Ge
Si
W/W_BH
.94 (Ir)
.50 (W, Re)
.32 (Os)
.17 (Ta)
T = 100 K
10 GeV
ħω [GeV]

Fig. 3

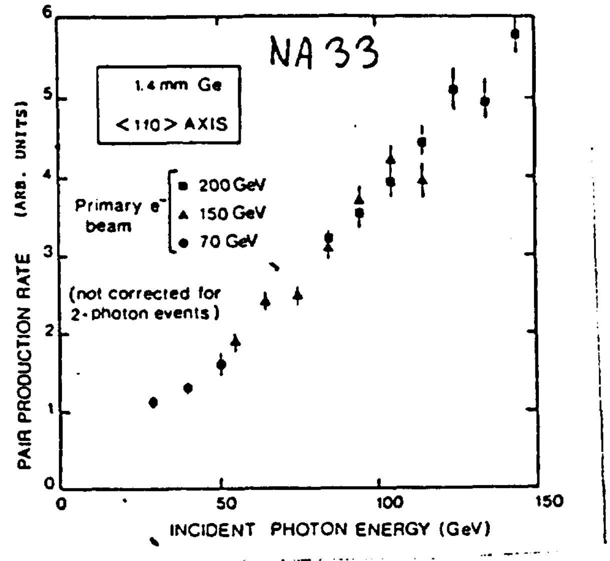
NA 33
1.4 mm Ge
<110> AXIS
Primary e⁻ beam
200 GeV
150 GeV
70 GeV
(not corrected for 2-photon events)
PAIR PRODUCTION RATE (ARB. UNITS)
INCIDENT PHOTON ENERGY (GeV)
0
1
2
3
4
5
6
50
100
150

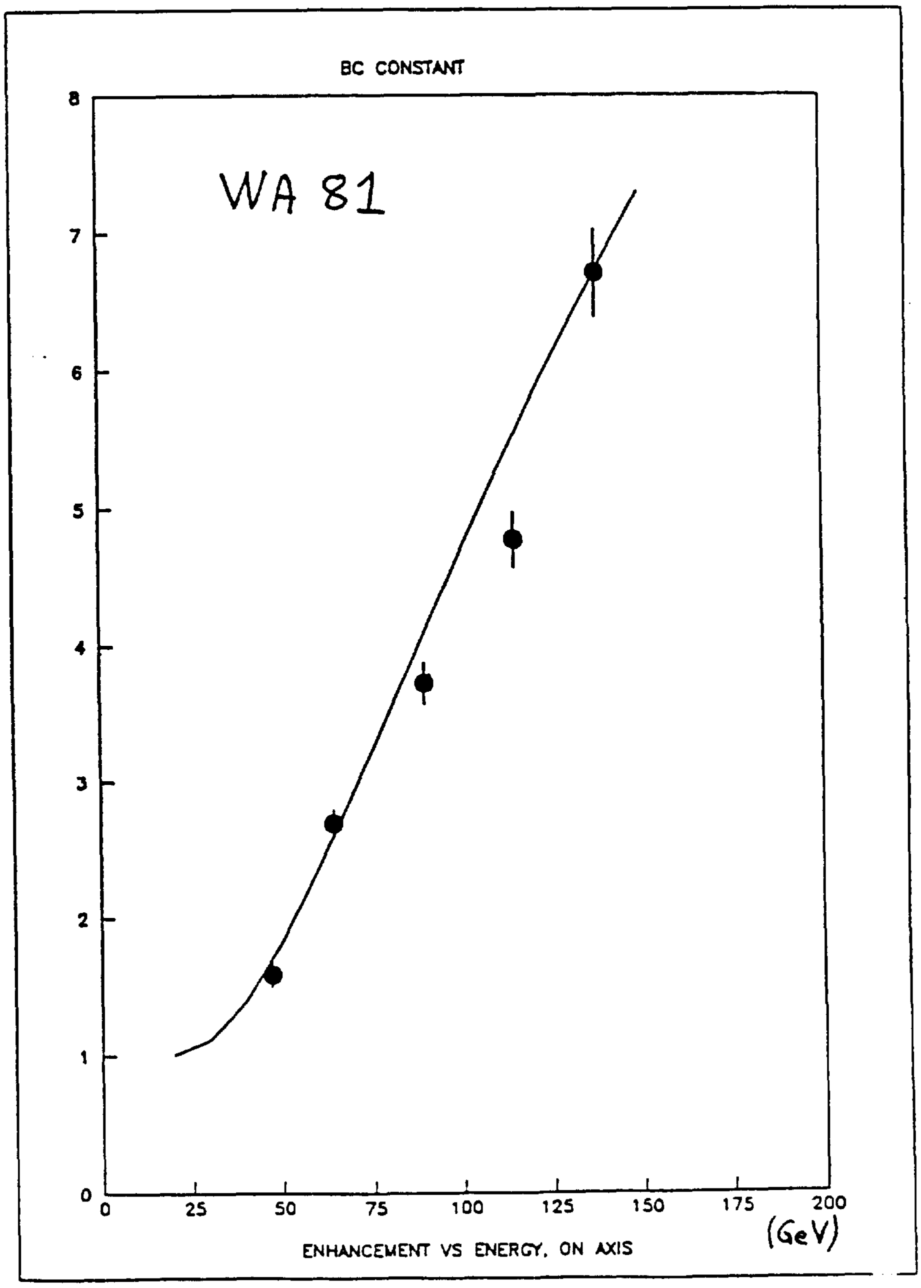
BC CONSTANT
WA 81
ENHANCEMENT VS ENERGY, ON AXIS
(GeV)
0
1
2
3
4
5
6
7
8
25
50
75
100
125
150
175
200

Fig. 4

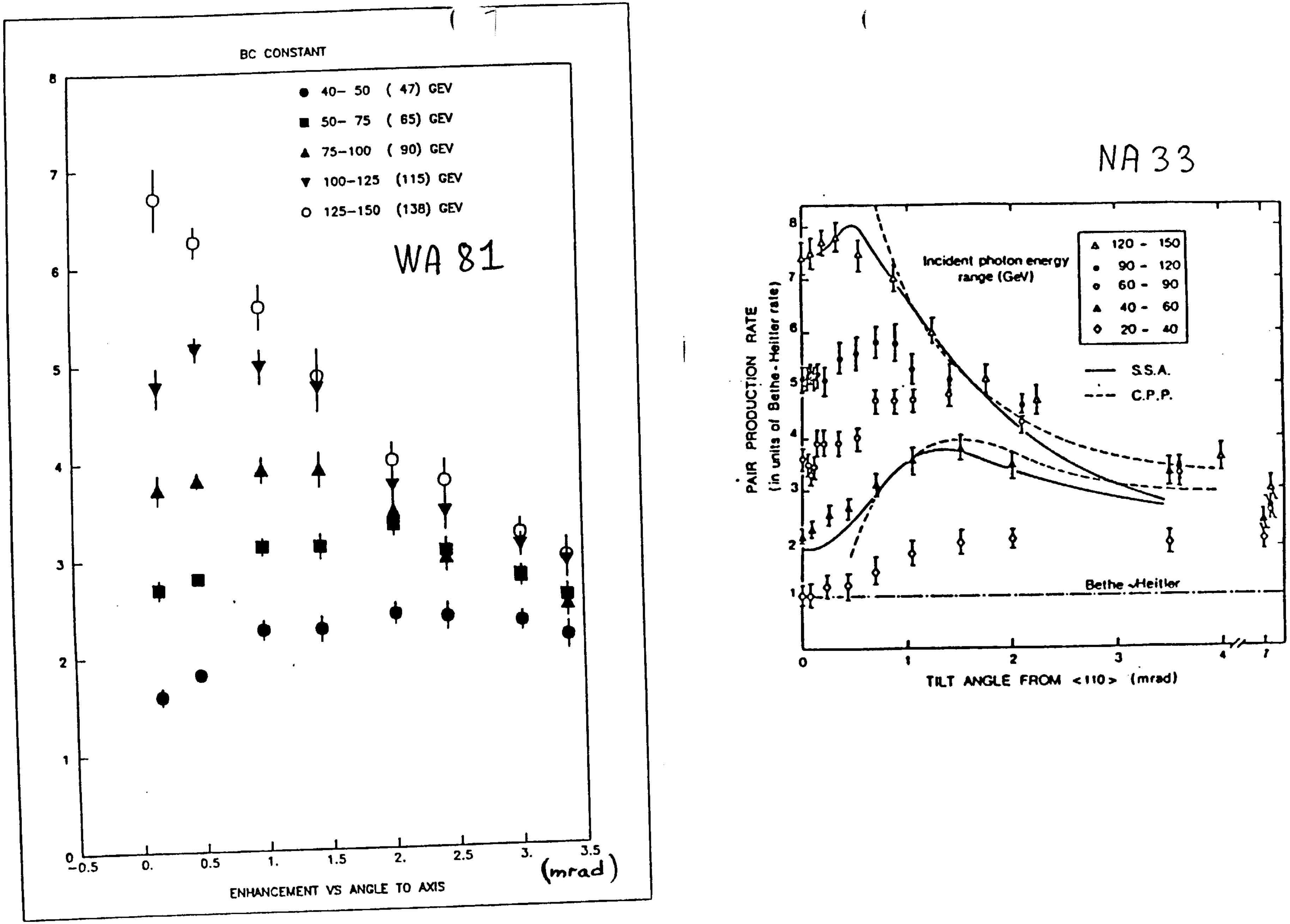
BC CONSTANT
● 40– 50 (47) GEV
■ 50– 75 (65) GEV
▲ 75–100 (90) GEV
▼ 100–125 (115) GEV
○ 125–150 (138) GEV
WA 81
(mrad)
ENHANCEMENT VS ANGLE TO AXIS
NA 33
PAIR PRODUCTION RATE
(in units of Bethe-Heitler rate)
Incident photon energy range (GeV)
120 - 150
90 - 120
60 - 90
40 - 60
20 - 40
S.S.A.
C.P.P.
Bethe-Heitler
TILT ANGLE FROM <110> (mrad)

Fig. 5

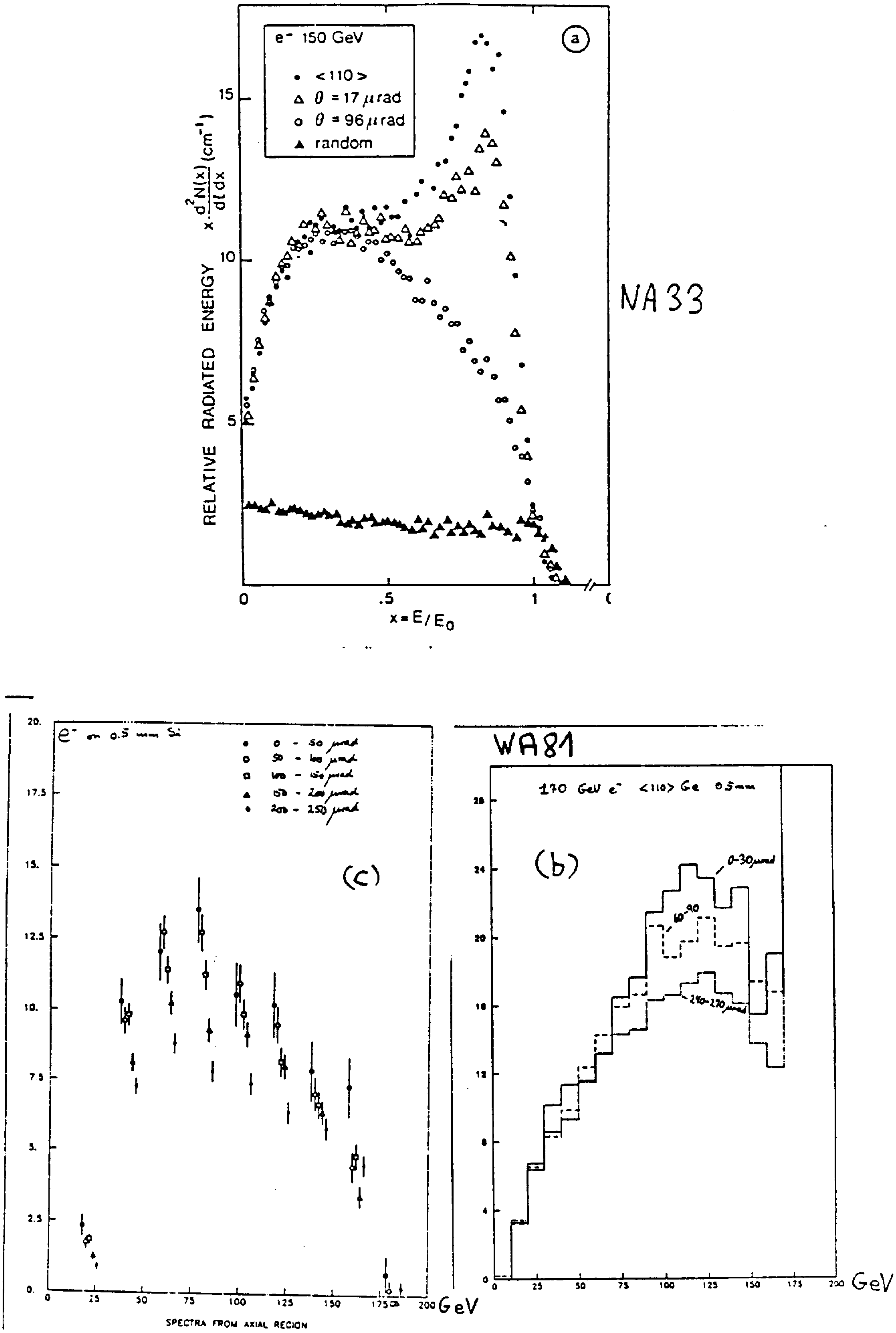

e⁻ 150 GeV
<110>
θ = 17 μrad
θ = 96 μrad
random
a
RELATIVE RADIATED ENERGY $x \cdot \frac{d^2N(x)}{dl\,dx}$ (cm⁻¹)
x = E/E₀
NA 33
e⁻ on 0.5 mm Si
0 - 50 μrad
50 - 100 μrad
100 - 150 μrad
150 - 200 μrad
200 - 250 μrad
(c)
SPECTRA FROM AXIAL REGION
GeV
WA81
170 GeV e⁻ <110> Ge 0.5mm
(b)
0-30 μrad
60-90
240-270 μrad
GeV

Fig. 6

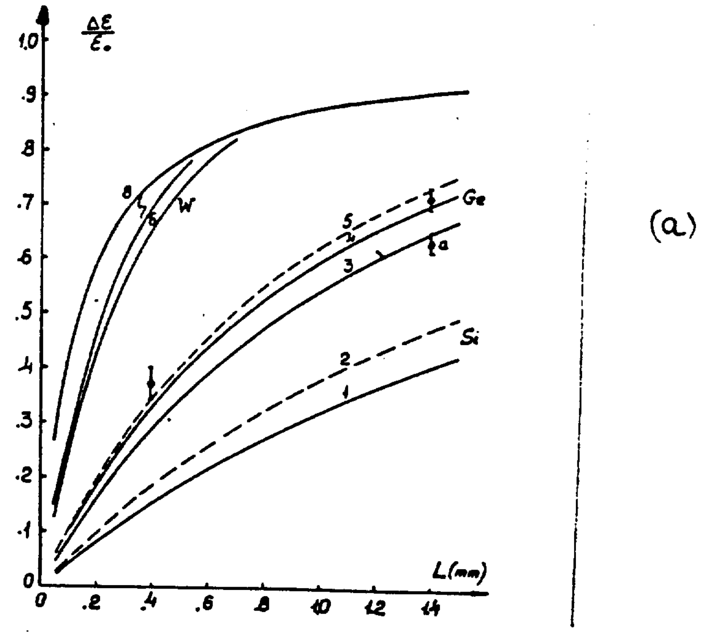
ΔE/E₀
1,0
.9
.8
.7
.6
.5
.4
.3
.2
.1
0
.2
.4
.6
.8
1.0
1.2
1.4
L(mm)
W
Ge
Si
(a)

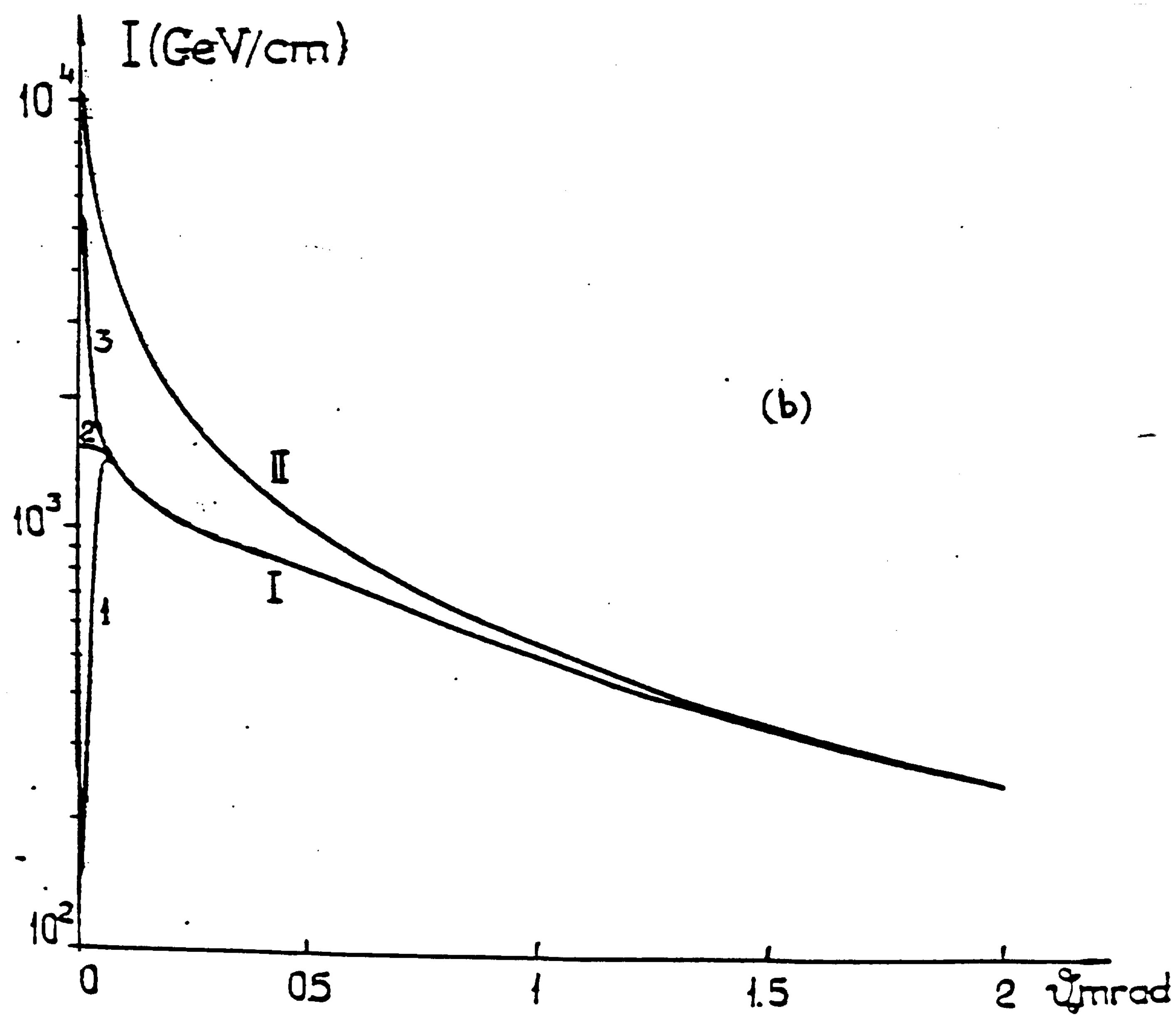
I (GeV/cm)
10^4
10^3
10^2
3
2
1
II
I
(b)
0
0.5
1
1.5
2
ϑ mrad

Fig. 7

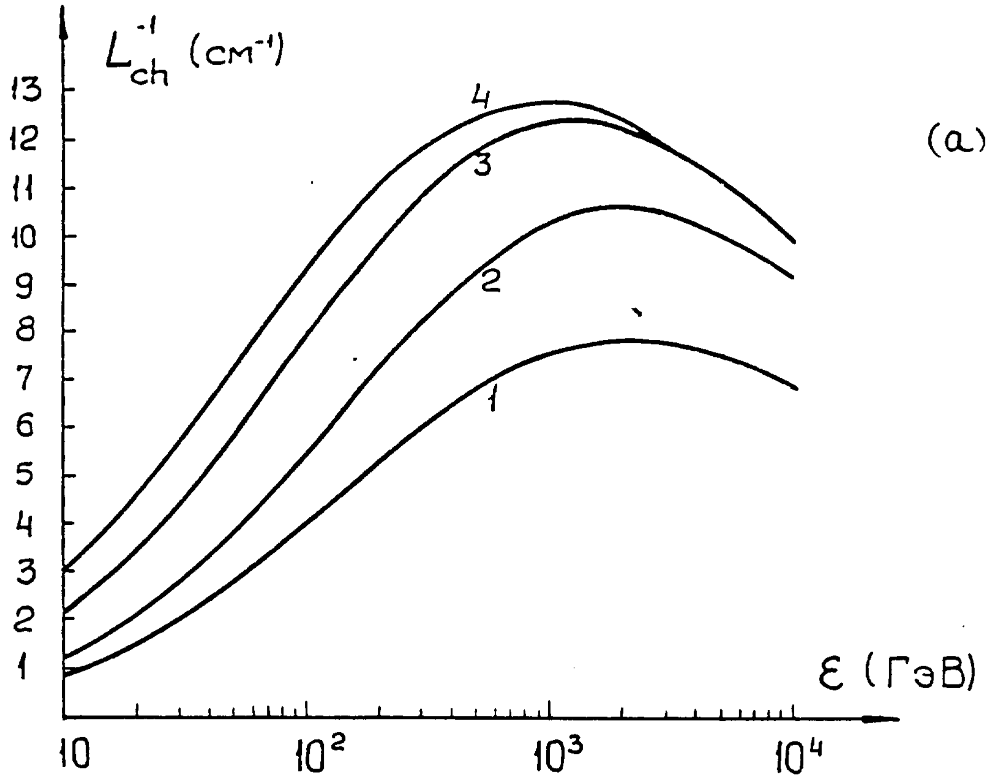

L_{ch}^{-1} (см$^{-1}$)
(a)
1
2
3
4
13
12
11
10
9
8
7
6
5
4
3
2
1
ε (ГэВ)
10
10^2
10^3
10^4

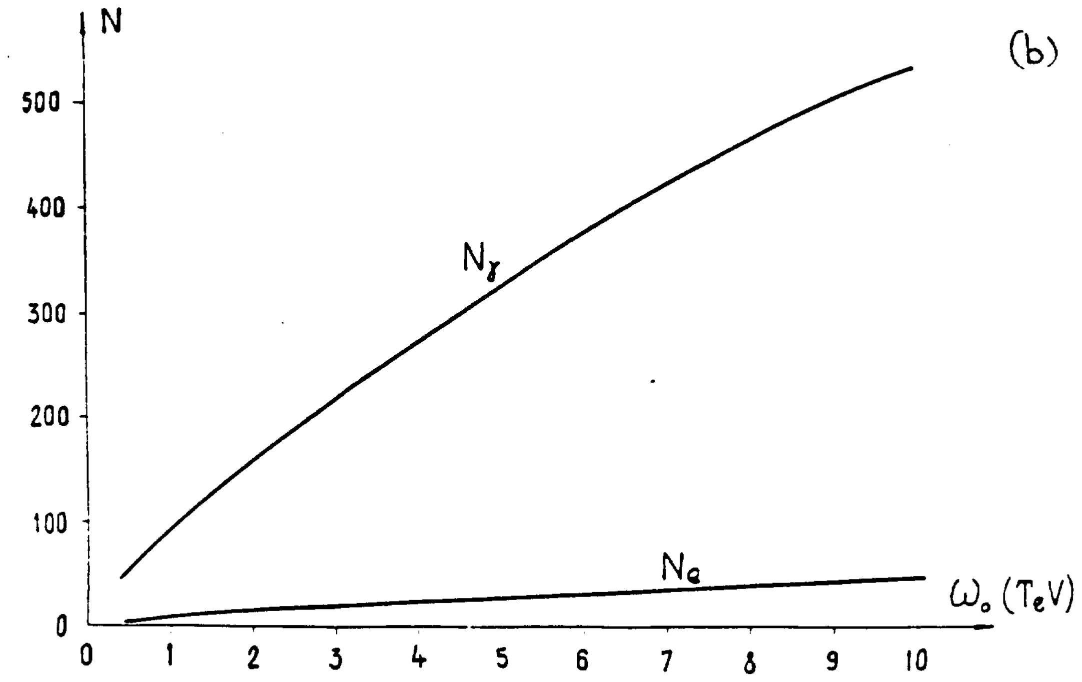

N
(b)
N_γ
N_e
ω_o (TeV)
500
400
300
200
100
0
0
1
2
3
4
5
6
7
8
9
10

Fig. 8

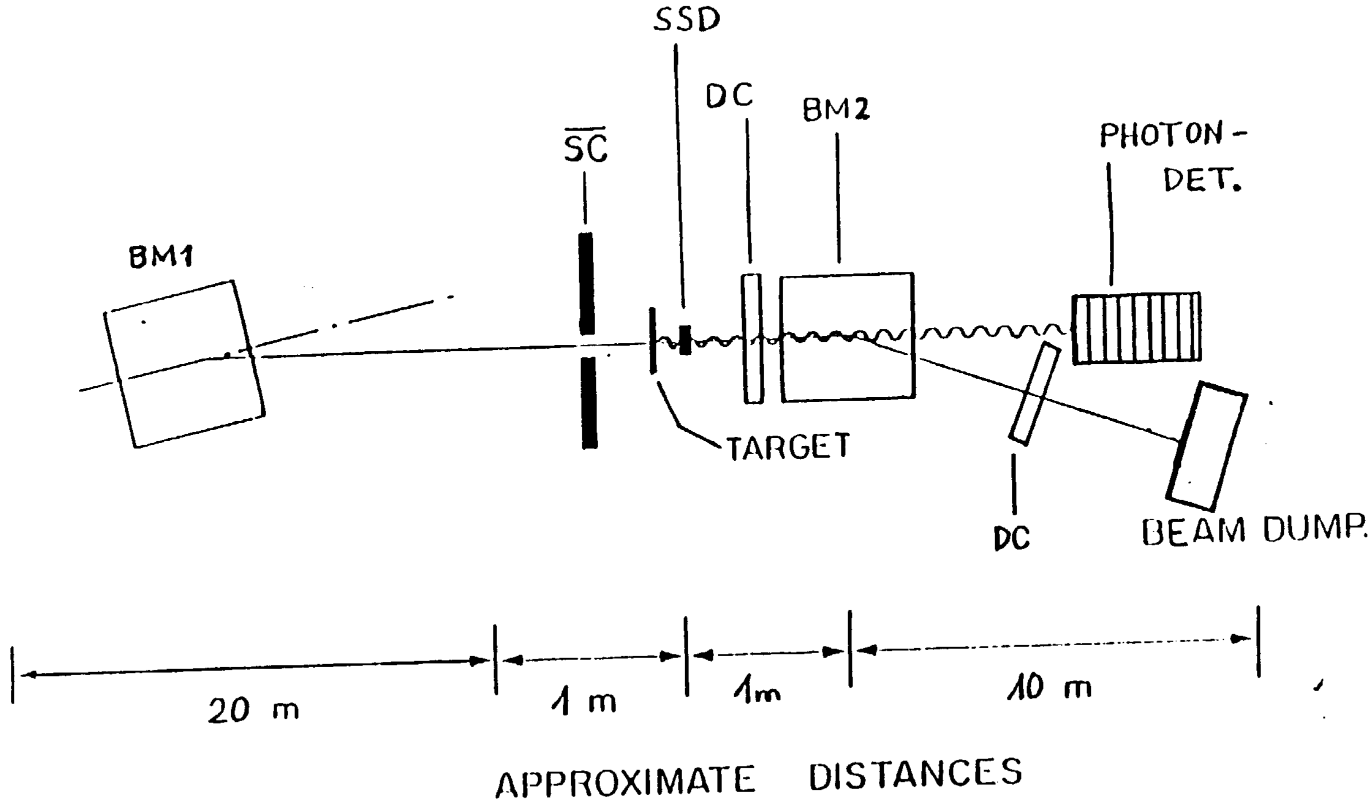
SSD
DC
BM2
$\overline{SC}$
PHOTON-
DET.
BM1
TARGET
DC
BEAM DUMP.
20 m
1 m
1m
10 m
APPROXIMATE DISTANCES

Fig. 9

High-energy physics

Particle production in crystals

Allan H. Sørensen and Erik Uggerhøj

ENERGETIC photons may convert into electron–positron pairs, but only in the presence of an external electromagnetic field — a process called pair production. Often the strong field inside an atom is exploited. Recently, Belkacem *et al.*[1] have demonstrated experimentally that a single crystal provides a very efficient alternative source of field. At a photon energy of 150 GeV, the photo-conversion probability in a germanium sample increases by a factor of about 10, to 0.3 mm^{-1}, if the incident beam is aligned within about 1 mrad of a major crystallographic axis. This effect could be used[2,3] in novel GeV γ-ray telescopes with high angular resolution, that ould be mounted in satellites.

The basic mechanism responsible for conversion of a photon into a particle–antiparticle pair is identical to that enabling a charged particle moving in an external field to emit electromagnetic radiation (Fig. 1). For the latter case, arguments of classical physics suggest that the radiation power is essentially proportional to the square of the product $(E/mc^2)\times Fm^{-1}$ where E is the particle energy, m is the rest-mass, F is the force acting on the particle and c is the speed of light. This implies increased intensities for high energies, strong fields and light particles. With laboratory fields and beam energies available now, the radiation is confined to relatively 'soft' photons, with energy orders of magnitude less than that of the projectile, even using light electrons. For example, synchrotron radiation facilities with GeV particles produce keV photons. Atomic fields, however, are sufficiently strong that a penetrating energetic electron is able to radiate all its kinetic energy into a photon. In pair creation, 'hard' photons are involved as all the primary energy is transferred to the electron and the positron. Hence, pair creation is essentially impossible in laboratory fields whereas it is perfectly possible in atomic fields.

But why should a group of regularly arranged atoms (a single crystal) be introduced as the source of field? The keyword is coherence. Coherent action of crystal atoms is well known from 'channelling' phenomena as we described in a recent review[4]. Consider a charged particle impinging at a small angle on a row of atoms. Such a projectile is subjected to many correlated, soft collisions. The row acts as a whole and the resulting trajectory is essentially identical to the one obtained using a 'continuum' string obtained by smearing the atomic charges uniformly along the row. The strength of the transverse field is of the order of 10^{11} V cm^{-1}.

The coherence in scattering observed at small impact angle also enhances the emitted radiation[5]. The emission of photons by electrons traversing the field of a row of atoms is stronger than if the atoms were distributed randomly. (A classical analogue is constructive interference of radiation emitted at successive scattering centres.) The enhancement obtained is up to two orders of magnitude. For impact energies in the range MeV–GeV, this enhancement is found only for soft photons. In the 100-GeV range, however, the coherent magnification extends to photons with the projectile energy. Conversely, for low impact-angle photons in the 100-GeV range, the probability of photo-conversion into electron–positron pairs is enhanced (Fig. 2*a*).

The pair-production rates recorded recently by Belkacem *et al.*[1] agree nicely with theoretical predictions. This holds true for the variation with decisive parameters like photon energy and angle to crystal axis. Also the agreement on an absolute scale is quite satisfactory. The discrepancies with theory encountered in previous data[5] have been eliminated. For photons incident parallel to a crystal axis, the theory developed[6] for pair creation in strong (homogenous and macroscopic) electromagnetic fields is applicable. Consequently, the experiment can be considered a successful proof both of the significant influence of crystal structure at high energies and of strong-field quantum electrodynamics. The dependence of the effect on target material and temperature, and on the energy of one of the produced particles, is yet to be studied.

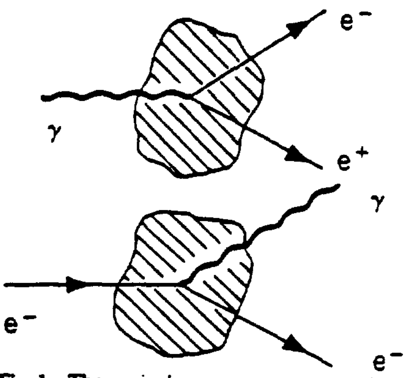

Fig. 1 The equivalent processes, conversion of a photon (γ) into an electron (e^-)–positron (e^+) pair, and photon emission by an electron. Shaded regions symbolize the external field.

Along with pair creation, Belkacem *et al.* have also measured photon emission by 150-GeV electrons and positrons incident near an axial direction in a germanium crystal[7]. Strong enhancements are observed for alignments better than 1 mrad. At very small angles, ≤0.05 mrad, electrons get focused around the axis whereby they give higher yields and photon energies than do positrons, which are defocused (Fig. 2*b*). For electron impact, however, the increase in yield observed below 0.05 mrad is gathered in a strong photon peak at 85 per cent of the primary energy. No explanation has been given for this phenomenon. Further experiments on very thin samples are urgently awaited to decide whether a new effect is responsible or if the origin of the peak is trivial, for example caused by two or more photons radiated by a given electron being recorded as one of energy equal to their sum. We have estimated the variation in the total radiated energy at angles ≤0.05 mrad (Fig. 2*b*) and found

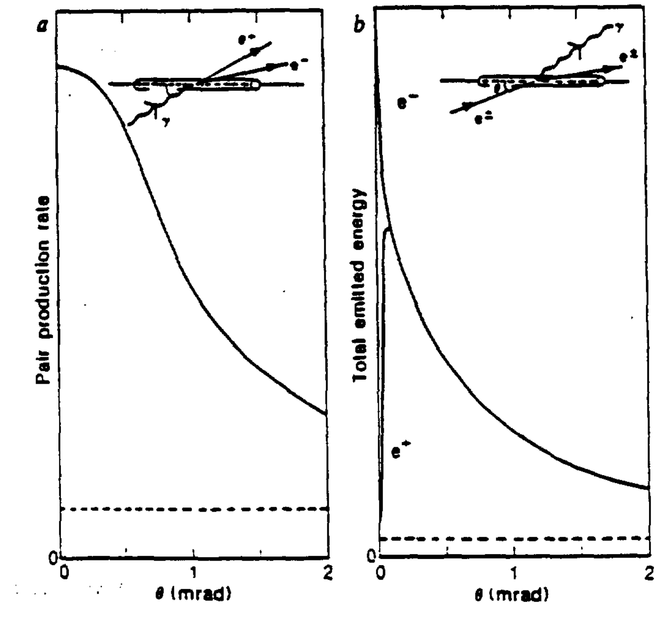

Fig. 2 *a*, Pair-production rate and *b*, photon emission as functions of incidence-angle θ relative to a row of a continuum crystal (inserts) for impact in the 100-GeV region. Dashed lines indicate the level obtained far from axes (and planes). The coherent action of the crystal, as manifested through the macroscopic continuum rows, leads to strong enhancement at small angles.

good agreement with the observations.

Recently, our own group has performed experiments at CERN similar to those reported in refs 1 and 7. For pair creation, the results confirm those of Belkacem *et al.*[1]. For radiation, preliminary analysis of data for electrons penetrating a very thin silicon crystal reveals a further increase in the yield for impact closer than 0.05 mrad to the axis, as reported in ref. 7. Unfortunately, it is not possible to draw a conclusion on the occurrence of a hard-photon peak because of poor counting statistics.

Finally, are there any applications? We have mentioned above the possibility of direction-sensitive, hard-photon detectors[2,3]. An energetic (≥100-GeV) photon has a high probability of pair-production in a 2–3-mm-thick germanium crystal, provided it enters within about 1 mrad to a major axis. This feature could be exploited to improve, by several orders of magnitude, the angular resolution in locating hard-photon sources in the Universe. A very simple piece of equipment is obtained if the converting crystal itself is a solid-state detector measuring the conversion rate. Also, coherence in crystals could enhance the intensity of particle beams produced in high-energy laboratories. Both applications depend on the development of a cascade — a succession of the processes shown in Fig. 1, by which a single, high-energy photon converts into many low-energy photons, electrons and positrons. At high impact energies, cascades develop fully in approximately 1 cm of aligned germanium, whereas 10–50 times more non-aligned material is needed: tests with thick aligned samples were performed some years ago[8]. The use of tungsten rather than germanium would extend the useful range to lower photon energies. ☐

1. Belkacem, A. *et al. Phys. Rev. Lett.* 58, 1196–1199 (1987).
2. McBreen, B. *Astr. Express* 1, 105–109 (1984).
3. Baier, V.N., Katkov, V.M. & Strakhovenko, V.M. *Nucl. Instrum. Meth.* A250, 514–517 (1986).
4. Sørensen, A.H. & Uggerhøj, E. *Nature* 325, 311–318 (1987).
5. Belkacem, A. *et al. Phys. Rev. Lett.* 53, 2371–2373 (1984); erratum 54, 852 (1985).
6. Erber, T. *Rev. mod. Phys.* 38, 626–659 (1966).
7. Belkacem, A *et al. Phys. Lett.* B177, 211–216 (1986).
8. Del Fabbro, R. & Murtas, G.P. *Phys. Scr.* 23, 690–696 (1981).

Allan Sørensen and Erik Uggerhøj are at the Institute of Physics, University of Aarhus, DK-8000 Aarhus C, Denmark.

Plate tectonics

Drifting mantle hotspots

Peter Olson

PLATE-TECTONIC motions have erased nearly every coordinate system capable of determining the absolute location on the Earth's surface of past geological events. Two terrestrial reference frames not obviously affected by seafloor spreading are the main geomagnetic field, whose time-averaged state is nearly a geocentric, axial dipole; and the mantle hotspots, long-lived centres of volcanic activity thought to be fixed with respect to each other. Now, even these reference frames, particularly the hotspots, appear to be mobile, according to results presented by Sager and Bleil[1], and by Molnar and Stock on page 587 of this issue[2].

J.T. Wilson[3] was the first to recognize that certain chains of volcanic islands such as Hawaii show a progressive increase in age in the direction of plate motion and seem to be tracks originating from localized hotspots fixed in the mantle beneath the plate. W.J. Morgan[4] established their importance in geodynamics, proposing that hotspots are stationary with respect to each other and define an irregular, rigid reference frame; and that they result from thermal plumes rising from deep in the mantle (see figure). The first point — the fixity hypothesis — can be tested by reconstructions of past plate movements. Early studies, based either on global datasets for the past 10 million years (Myr) or older data from slow-moving plates, generally supported the concept of fixity, showing little or no deviation between plate trajectories and hotspot tracks. This indicated that the source of hotspots, the deep mantle, must remain virtually undeformed while the lithospheric plates and the upper mantle circulate above it. But this rather simple picture conflicts with recent results from seismic tomography that show large-scale lateral heterogeneity in the lower mantle[5] and undulations of ± 6 km in the core–mantle boundary[6], both strong indicators of vigorous convection in the lower mantle. Large-scale convection in the source region should cause plumes to drift and make hotspots move with respect to both the plate above and the hotspots under adjacent plates. The contradiction would be resolved if hotspots do move about in the mantle, but more slowly than the sea floor typically spreads. On kinematic grounds the apparent drift of a hotspot produced by a deep plume should be sensitive to the net sublithospheric velocity in the vertical cross-section of the mantle through which the plume ascends, which would be small compared with the plate velocity and might be nearly in the opposite direction.

To resolve small relative motion (millimetres per year), old hotspot tracks on fast-moving plates must be used, and that is the approach of Sager and Bleil, and of Molnar and Stock, using essentially independent methods. Sager and Bleil use palaeolatitude determintions derived from Deep Sea Drilling Project cores from the western Pacific to show that the geomagnetic latitude of the Hawaiian hotspot has decreased at a rate of about 0.3° Myr^{-1} between 70 and 40 Myr ago. During this time the Pacific plate moved north and the Hawaiian hotspot was producing the Emperor Sea Mounts. As palaeomagnetic data of this type do not resolve changes in longitude, only changes in hotspot latitude can be determined using Sager and Bleil's approach. Also, because their comparison is based on the position of a single hotspot relative to the geomagnetic pole, some ambiguity enters when interpreting their results. For example, the relative motion could partly result from drift of the geomagnetic dipole, rather than just the hotspot. Theoretical arguments, supported by extensive palaeomagnetic data from the recent past, strongly indicate that the main dipole field tends to align along the Earth's axis of rotation, so that motion of the geomagnetic pole is tantamount to motion of the axis relative to surface features. This is called true polar wander (TPW) and there is some evidence that this has occurred to a few degrees of latitude over the past 40 Myr. Sager and Bleil show that TPW, with the spin axis moving away from the Pacific Basin, can explain their results.

But from a geodynamical point of view, a more likely explanation is that the hotspots are moving. A direct test of this alternative has been made by Molnar and Stock, without making any direct appeal to the positions of the palaeomagnetic pole. These authors show results of a detailed comparison between the tracks of Hawaii and hotspots in other oceans with their predicted tracks, calculated using the

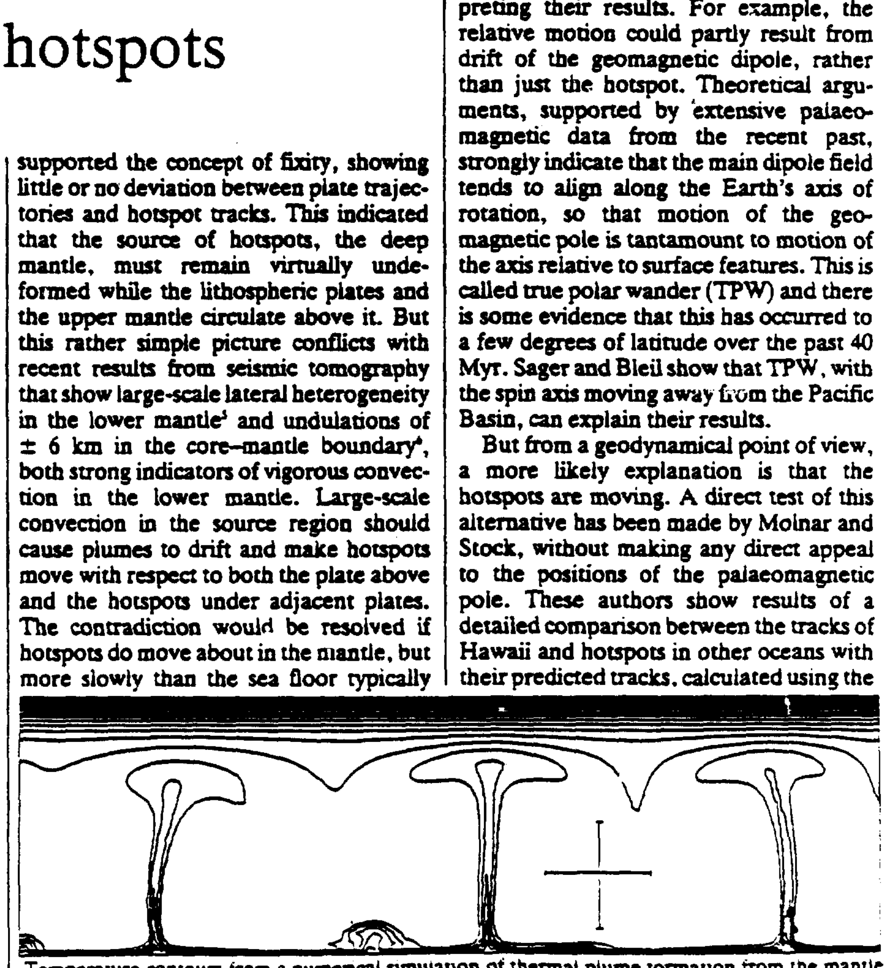

Temperature contours from a numerical simulation of thermal plume formation from the mantle D″ thermal-boundary layer and hotspot formation by interaction with the lithosphere. The scale-bars are 200 km (horizontal) and 100 km (vertical). (Courtesy of G. Schubert and C. Anderson.)